Two Intermediates Appear on the Lumirhodopsin Time Scale after Rhodopsin Photoexcitation†

Istvan Szundi, James W. Lewis, and David S. Kliger*

Department of Chemistry and Biochemistry, University of California, Santa Cruz, Santa Cruz, California 95064

Received December 10, 2002; Revised Manuscript Received February 18, 2003

ABSTRACT: Absorbance difference spectra were recorded at 20 °C with a dense sequence of delay times from 1 to 128 μs after photolysis of lauryl maltoside suspensions of rhodopsin prepared from hypotonically washed bovine rod outer segments. Data were best fit by two-exponential components with a small, fast component ($\tau = 12$ μs) occurring during the period that lumirhodopsin has been presumed to be stable. The shape of the spectral change corresponds to an ~2 nm red shift of the lumirhodopsin spectrum. Measurements with linearly polarized light verified that no absorbance changes associated with rotational diffusion were present in these preparations on this time scale, and experiments designed to enhance isorhodopsin production during photolysis showed no effect on the relative amplitude of the fast process. A similar process was previously observed in membrane suspensions of rhodopsin, but there the similarity of the change to rotational diffusion artifacts made conclusive identification of a second lumirhodopsin difficult. However, reexamination of polarized light measurements on rhodopsin in membrane supports the fact that the fast process seen here in detergent also takes place there. The new absorbance process occurs when time-resolved resonance Raman experiments have shown that the protonated Schiff base is moving from one hydrogen bond acceptor to another. The results are discussed in the context of possibly related processes on the same time scale that have been observed recently in artificial visual pigments with synthetic retinylidene chromophores and in a related rhodopsin mutant. The details of lumirhodopsin behavior are important because it is the last protonated Schiff base intermediate that occurs under physiological conditions.

As the trigger of the visual process, the mechanism of rhodopsin activation has been a topic of interest for many years. More recently, it has gained added significance because rhodopsin activation provides unique insights about related proteins in the family of G-protein-coupled receptors which are of great interest but more difficult to study. The revelations of the crystal structure of rhodopsin (*1*−*3*) have provided a concrete framework within which to interpret time-resolved measurements of the activation process with the goal of gaining information about the structures of photointermediates which occur on the pathway to activation. Some photoexcitation intermediates were originally detected in low-temperature absorbance measurements (*4*), but others which cannot be thermally trapped can only be seen in near-physiological temperature, time-resolved absorbance measurements (*5*, *6*) or time-resolved resonance Raman experiments (*7*). Resonance Raman and absorbance measurements are complementary techniques in that the excellent time resolution and signal-to-noise ratio attainable with absorbance allow the presence and stability range of new intermediates to be determined, while the higher information content of resonance Raman spectroscopy can provide structural insight when applied to a well-characterized mixture of intermediates.

Two of the nonthermally trappable photoexcitation intermediates flank lumirhodopsin (Lumi).[1] One of these, the blue-shifted intermediate (BSI), decays to form Lumi, and the other nonthermally trappable intermediate, Meta I_{380}, is produced by one branch of Lumi decay near physiological temperatures. Lumi itself seemed to be an island of stability with its formation rate being at least 2 orders of magnitude greater than its decay rate. That apparent stability was in contrast to the results of recent photolabeling experiments which indicated that a large change in the position of the β-ionone ring had taken place at the Lumi stage (*8*). Other evidence from artificial pigments derived from synthetic analogues of retinal and rhodopsin mutants also suggested that change could occur during the time normally associated with Lumi stability (*9*, *10*). Measurements on membrane suspensions of rhodopsin showed small absorbance changes during the time that Lumi was presumed stable, but these had a shape and time constant, ~5 μs (*11*), generally consistent with rotational diffusion of rhodopsin in the disk membrane. Because of this similarity and the fact that scattering of actinic laser light by membranes breaks down cylindrical symmetry, potentially allowing rotational diffusion to produce a signal even in properly polarization averaged or magic angle absorbance data, the changes seen

† This work was supported by Grant EY00983 from the National Eye Institute of the National Institutes of Health (to D.S.K.).

* To whom correspondence should be addressed. Telephone: (831) 459-2106. Fax: (831) 459-4136. E-mail: kliger@chemistry.ucsc.edu.

[1] Abbreviations: BSI, blue-shifted intermediate; LM, lauryl maltoside; Lumi, lumirhodopsin; Meta, metarhodopsin; PSB, protonated Schiff base; ROS, rod outer segment; Tris, tris(hydroxymethyl)-aminomethane.

10.1021/bi0206964 CCC: $25.00
Published on Web 04/11/2003

in membrane suspensions were not interpreted in terms of two Lumi intermediates (*12*).

Since the original careful characterization of rhodopsin activation in membrane suspension (*6*) a good deal of effort has gone into elucidating the mechanism of rhodopsin decay in detergent suspensions (*13*), primarily because rhodopsin mutants are purified in that form (*14*). The results have shown that the same general mechanism prevails in detergent-solubilized and membrane samples, albeit with significantly perturbed rate constants. The work reported here takes advantage of the fact that rotational diffusion in detergent suspensions is orders of magnitude faster than it is in membrane so that time-resolved absorbance studies of Lumi stability can be carried out free from possible rotational diffusion artifacts. These careful studies show a small red shift in the Lumi absorbance spectrum on the 10 μs time scale at 20 °C which cannot arise from rotational diffusion. Consideration of the details of polarized absorbance measurements previously obtained from membrane suspensions shows that a similar evolution of Lumi must be taking place there. The shape of the spectral change is similar but not identical to the Lumi minus rhodopsin difference spectrum which would result from rotational diffusion. Similarities in shape and time constant of the Lumi spectral evolution to those expected from a rotational diffusion artifact are an unfortunate coincidence which acted in concert with the small size of this spectral change relative to others in the rhodopsin bleaching sequence to make definite detection difficult. However, in the context of recent resonance Raman measurements which show Lumi to have broken its protonated Schiff base (PSB) hydrogen bond (*7*) and that the migration to a new hydrogen bond acceptor may be more complex than originally thought, it is an exciting development.

MATERIALS AND METHODS

Preparation of Rhodopsin Samples. Rod outer segments (ROS) were prepared as described previously (*6*) from frozen bovine retinas (J. A. Lawson, Omaha, NE). Extrinsic membrane proteins were removed from ROS by hypotonic washing with pH 7.0, 1 mM EDTA solution, followed by a single wash with TBS (10 mM Tris, 60 mM KCl, 30 mM NaCl, 2 mM $MgCl_2$, 0.1 mM EDTA, pH 7.0), and the final pellet after centrifugation was resuspended in either 1% or 5% lauryl maltoside (LM) detergent in TBS so that the final rhodopsin concentration was 1 mg/mL. Immediately prior to optical measurements any sedimentable material was removed by centrifugation, and samples were degassed at room temperature by gently agitating them under vacuum.

Collection of Time-Resolved Absorbance Difference Spectra. Individual 1 μL samples were photolyzed at 20 °C by 7 ns (fwhm) laser pulses from a dye laser, pumped by the 355 nm third harmonic of a Nd:YAG laser that produced vertically polarized 477 nm light. The energy delivered to the sample was 80 $\mu J/mm^2$. The change in absorption spectrum at a particular time delay, ranging from 1 to 128 μs after photolysis, was measured using a gated optical multichannel analyzer (*15*). Absorbance changes were monitored perpendicularly to the excitation beam using a flashlamp that produced white light polarized at 54.7° relative to the laser polarization direction. The path lengths of the actinic light and probe light in the sample were 0.5 and 2 mm, respectively. To verify that an oriented distribution of chromophores did not exist during these measurements, absorbance difference spectra were collected at 1 μs after photoexcitation for comparison using vertically and horizontally linearly polarized probe light. To determine whether isorhodopsin production influenced (or accounted for) kinetic components, experiments were conducted as above except that, instead of 477 nm excitation, a pulse of 540 nm light from an optical parametric oscillator pumped by the 355 nm third harmonic of a Nd:YAG laser was used.

Data Analysis. The set of experimental difference spectra, $\{\Delta A(\lambda,t)\}$, were analyzed by singular value decomposition (svd) and global exponential fitting (*5*). In svd the data matrix, $\Delta\mathbf{A}$, is split into a product of three matrices: $\Delta\mathbf{A} = \mathbf{U}\cdot\mathbf{S}\cdot\mathbf{V}'$, where **U** is a matrix of orthogonal spectral vectors, **V** is their time dependence, and **S** contains the significance values indicative of the contributions of the **U** and **V** vectors to the experimental data. The significant vectors in the temporal matrix, **V**, are fitted to a sum of exponential functions followed by calculation of the spectral amplitudes, the b-spectra. From the b-spectra and exponential functions the matrix of reproduced data, $\Delta\mathbf{a}$, is calculated:

$$\Delta a(\lambda,t) \equiv b_0(\lambda) + b_1(\lambda)\exp(-t/\tau_1) + b_2(\lambda)\exp(-t/\tau_2) + \ldots$$

where the τ_i are the apparent lifetimes and the $b_i(\lambda)$ are b-spectra corresponding to difference spectra which decay with the associated lifetime. The difference between the experimental data matrix and the reproduced data, $\mathbf{R} = \Delta\mathbf{A} - \Delta\mathbf{a}$, gives the matrix of residuals that is used to judge the quality of the fit. The residual matrix of an adequate fit contains only featureless noise caused by the finite number of photons detected in each measurement. Equilibrium constants and, where appropriate, microscopic rate constants for specific mechanisms were determined by fitting the b-spectra using intermediate spectra as described previously (*16*).

RESULTS

Time-resolved absorbance difference spectra collected after photolysis of rhodopsin in LM suspension are shown in Figure 1. Data for detergent suspensions of rhodopsin on the time scale after photolysis studied here have previously been shown to be best described by a square scheme (*13*):

$$\begin{array}{ccccc} \ldots\ BSI & \rightarrow & \textbf{Lumi} & \underset{\mathbf{k_2}}{\overset{\mathbf{k_1}}{\rightleftharpoons}} & \textbf{Meta I}_{\mathbf{380}} \\ & & k_4 \downarrow & & \downarrow k_3 \\ & & \textit{Meta I}_{480} & \underset{k_6}{\overset{k_5}{\rightleftharpoons}} & \textit{Meta II}\ \ldots \end{array}$$

In the above version of the square scheme, the intermediates that do not appear appreciably on the time scale of the observations made here are shown in italics, and the single process that would be expected to be resolved by our measurements is shown in boldface type. The 215 ns lifetime observed for BSI decay (*5*) ensures that Lumi is fully formed within 1 μs, which is the time at which we collect our first absorbance difference spectrum. The expected product of

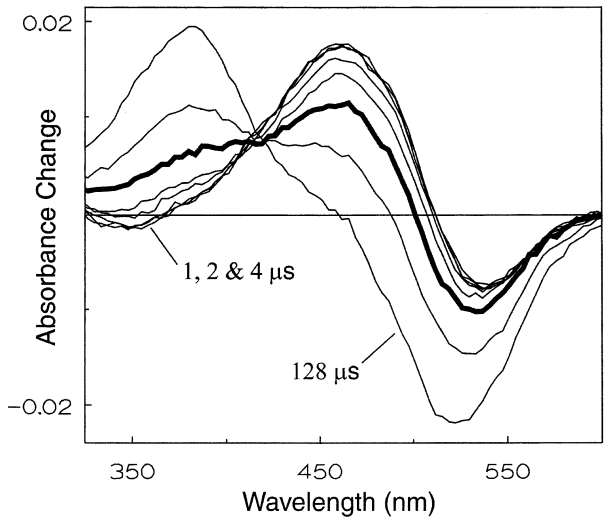

FIGURE 1: Time-resolved absorbance difference spectra of rhodopsin solubilized in 1% LM collected at delays of 1, 2, 4, 8, 16, 32, 64, and 128 μs after photolysis by a 7 ns pulse of 477 nm laser light. Data are the average of several experiments (90% confidence limits ± 0.0003). The thicker curve shows data collected at 32 μs. Direct evidence for a fast exponential process comes from the fact that the change from 1 to 32 μs near 450 nm is much greater than the change over the same time range near 530 nm while similar changes take place at these two wavelengths at later times. Data collected from rhodopsin solubilized in 5% LM were essentially identical to the data in this figure at early times (<32 μs), and later times showed a somewhat accelerated slow process with spectral shape nearly identical to that seen here in the 1% LM data.

Lumi decay is primarily Meta I_{380}, an intermediate which begins to appear above 20 °C in membrane suspensions of rhodopsin and whose formation is greatly favored by detergent as used here. The other branch containing Meta I_{480}, the classical metarhodopsin I intermediate, would be the principal path after photoexcitation of rhodopsin in membrane at 20 °C and below. The decay processes described by the two down arrows have time constants of hundreds of microseconds, so if they are detected at all here, they would be expected either to distort the spectral shape of the single main component or to produce a small, slow second component in the exponential fit.

Residuals from a single-exponential fit to data from both 1% and 5% LM suspensions of rhodopsin (Figure 2, top) show distinct curvature which is larger than the noise level for measurements at individual wavelengths. In 8 separate places, sequential wavelength residuals which are outside the 90% confidence limits appear with the same sign at least 8 times and in two places occur 18 times. The probability that a single sequence of 8 such similarly signed residuals would occur by chance is <0.01%. Further, as shown below, the shape of these residuals is not only evident in the averaged data but also highly correlated in the individual data sets within the average. Residuals from a two-exponential fit (Figure 2, middle) are flat, showing that two exponentials fit the data well. However, rather than adding a component slower than the main Lumi ⇌ Meta I_{380} process with a blue shift, such as might result from neglect of the formation of Meta I_{480} or Meta II, the b-spectra from the two-exponential fit (Figure 2, bottom) display an unexpected faster process with a 12 μs lifetime (1% LM, identical within uncertainty to the 13 μs lifetime detected in 5% LM) and a shape that indicates a small red shift in the Lumi spectrum.

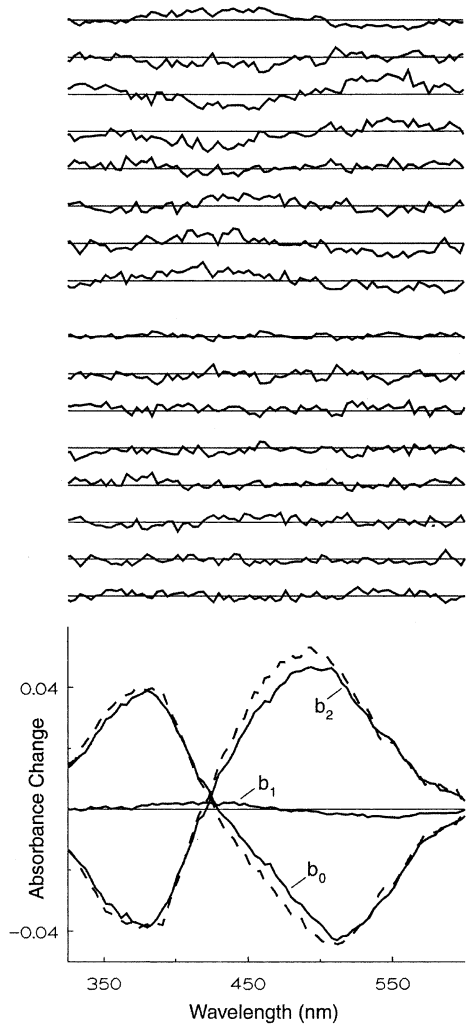

FIGURE 2: Top: Residuals obtained from the best single-exponential fit to the data in Figure 1 (1 μs residual at bottom, spacing 0.002 absorbance unit). Similarly shaped residuals were obtained for a single-exponential fit of data from 5% LM solubilized rhodopsin. Middle: Residuals obtained from the best two-exponential fit to the data in Figure 1. Similar results were obtained for 5% LM solubilized rhodopsin. Bottom: b-spectra obtained from two-exponential fits. The fast b-spectrum with exponential lifetime 12 μs, labeled b_1, was identical in the 1% and 5% LM samples, and so the average is plotted here. The time-independent component, b_0, and slower b-spectrum, b_2, differed with detergent concentration as shown [1% (—) lifetime = 180 μs; 5% (---) lifetime = 160 μs)].

The need for a process with a lifetime on the order of 10 μs in the fit was clearly apparent in the shape of the two most significant vectors in the temporal **V** matrix. The presence of this early exponential process is evident from a close examination of the data in Figure 1 even without fitting. There the different shape of absorbance changes from 1 to 32 μs compared to those seen from 32 to 128 μs and the small red shift in the isosbestic point at later times both give direct evidence for an early process taking place before Lumi decay gets underway. The larger, later process represented by b_2 is primarily the formation of Meta I_{380}. That process differs slightly at the two LM concentrations because addition of more detergent progressively forward shifts the Lumi ⇌ Meta I_{380} equilibrium, which is in agreement with our observation that the slow lifetime is shorter in 5% LM (160 μs) than it is in 1% LM (180 μs) although this difference may not be significant given the uncertainty in the determi-

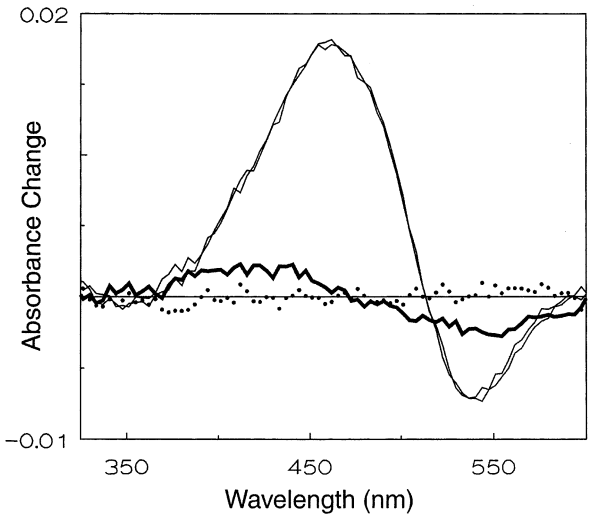

FIGURE 3: Polarized absorbance difference spectra collected at 1 μs after photolysis are shown as overlapping curves. Their difference is plotted as dots showing random scatter around the zero line. The time-dependent change observed to take place here on the time scale normally associated with Lumi stability, b_1, is also plotted (heavy line) for comparison with the Lumi minus rhodopsin difference spectrum (given by the 1 μs polarized data).

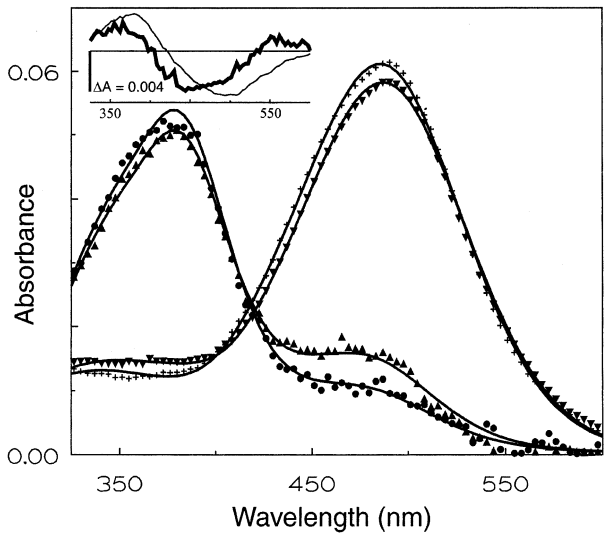

FIGURE 4: Absorption spectra of sequential intermediates. The first (+) and second (▼) sequential intermediates had spectra which were independent of detergent concentration within experimental uncertainty, and the average of all data are plotted for comparison with the fit (smooth curves) obtained from a model which assumes unidirectional conversion of the first form into the second. Imperfections in the fits of the smooth curves to the data are due to the fact that a simple set of model spectra were used. Note that the data presented in this figure are for the purpose of comparing Lumi I and Lumi II spectra, not for convincingly demonstrating their existence. The latter is best done on the basis of the difference spectra presented in Figures 1−3. The spectrum of the third sequential intermediate depended on detergent concentration, primarily due to the known forward shifting of the Lumi ⇌ Meta I_{380} equilibrium as more detergent is added. Data for 1% LM (▲) and 5% LM (●) are plotted separately. The experimental design was optimized to detect the two Lumi's, and hence the uncertainty in the third intermediate is larger. The bold line in the inset of the figure shows the difference spectrum between Lumi I and Lumi II, which is distinct from b_1 (which contains contributions from the much larger, slower process). For comparison, the fine line in the inset shows the difference between the third and second intermediates (1% LM) divided by ten.

nation of the slow lifetime here. Experiments conducted using 540 nm excitation (which produces several times more isorhodopsin than 477 nm excitation does) produced two time-dependent components with spectra and relative amplitudes (data not shown) similar to the results presented here for 477 nm excitation.

Absorbance changes at a delay of 1 μs measured using light linearly polarized parallel or perpendicular to the polarization direction of the actinic light are shown in Figure 3. These were identical and show that no linear dichroism existed at the earliest time delay studied here. The difference between the two polarized absorbances (plotted as dots) shows only noise which is small compared to the spectral change associated with the fast decay process, b_1 (plotted for comparison in the figure).

The absolute absorption spectra of sequential intermediates calculated from the 477 nm excitation data are shown in Figure 4. The first two intermediates' spectra were independent of LM concentration. Consistent with a detergent concentration dependence of the slow component lifetime, the spectrum of the third sequential intermediate shows a forward shift of the Lumi ⇌ Meta I_{380} equilibrium with increasing detergent concentration. As expected, due to the approximate nature of fitting Lumi decay with a single slower exponential, a small amount of the Meta I_{480} spectrum could be used to fit the third sequential intermediate spectrum. Data for the third intermediate are noisier than for the first two intermediates, and the shape of the third intermediate has the most uncertainty because the delay times were chosen here to maximize information about the early process. However, uncertainty in the spectral shape of the slow process has almost no effect on characterization of the fast process, and results for the slow process obtained here agree with more thorough characterization of Meta I_{380} formation and decay published elsewhere (*13*). The absorption maxima of the intermediates used in fitting were as follows: Lumi I, 488.5 nm; Lumi II, 490 nm; Meta I_{480}, 479 nm; and Meta I_{380}, 381 nm. The maximum of the bleach (which includes isorhodopsin formation) was 507 nm. Although these absorption maxima have an uncertainty of 2 nm due to the individual experiment calibration, the 1.5 nm shift in the spectrum of the second Lumi is more certain because it is based on differential measurements within individual experiments.

Residual Correlation for Separate Experiments. As discussed above, the vectors in the residual matrix of the single-exponential fit of the averaged data plotted against wavelength (top, Figure 2) displayed small but noticeable spectral features that could not be accounted for by experimental noise. The significance and reproducibility of the spectral information in the residuals were tested by calculating the correlation between the corresponding residual vectors of the individual experiments. The correlation parameters for two residual vectors, $\mathbf{R_1}$ and $\mathbf{R_2}$, taken at the same time delay but in different experiments, were calculated in the following way: $\mathbf{C_{12}} = \mathbf{(R_1 \cdot R_2)/(\langle R_1 \rangle \cdot \langle R_2 \rangle)}$, where the numerator represents the dot product of the two vectors and the denominator is the product of the lengths of the vectors. This formula gives a normalized measure of the correlation between $\mathbf{R_1}$ and $\mathbf{R_2}$: it will be equal to 1 if the two vectors point in exactly the same direction, −1 if they point in opposite directions, and 0 if they are completely randomly

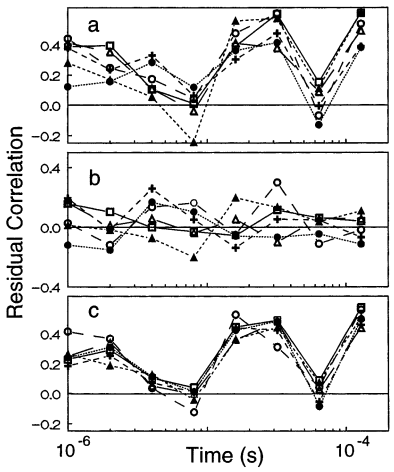

FIGURE 5: Correlation of temporal residuals for individual experimental series. Residual correlations (see text) taken pairwise among the four experimental series (two for 1% LM and two for 5% LM) are plotted for each time delay studied. (a) Single-exponential fit residual correlations show strongly correlated values for all delays except 8 and 64 μs. (b) Residual correlation for the two-exponential fit shows no correlation between any of the data sets at any delay time. Offsets which occur because of the single beam nature of our absorbance measurements are likely to contribute significantly to these amplitude correlations. (c) Single-exponential fit residual correlations after subtraction of two-exponential fit residual correlations show even more strongly correlated residuals displaying a distinctive shape.

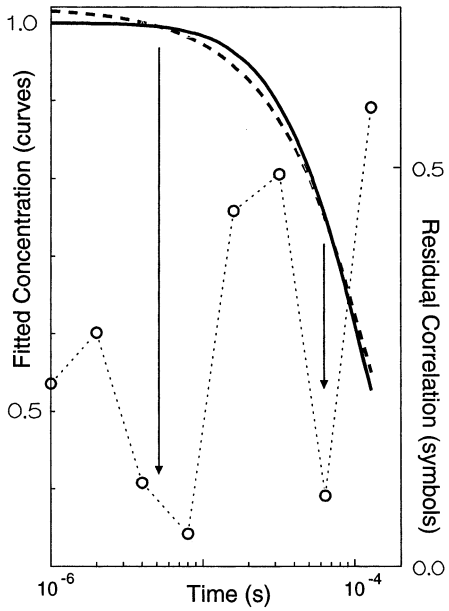

FIGURE 6: Origin of the shape occurring in residual correlation plots. The solid curve at the top shows the calculated concentration of an intermediate which decays in two consecutive steps with 12 and 180 μs lifetimes. The dashed curve superimposed on it shows the best single-exponential fit with a lifetime of 200 μs. The curves cross in two places, and at those times the single-exponential fit should have similar quality residuals to the two-exponential fit. The symbols in the lower part of the figure reproduce the residual correlations for two of the experimental series representative of the behavior shown in Figure 5, and as shown by the arrows, the minima in the correlation occur near the times predicted by the exponential simulation.

oriented. Because experimental noise is never perfectly random and there are small offsets in the residuals, the practical values of the correlation parameter are expected to take intermediate values. Four independent experimental series were compared: two conducted at 1% and two conducted at 5% detergent concentration (each series was comprised of ~100 data files each reporting on four photolysis measurements). The values of the correlation parameter for the residuals of the single-exponential fit are displayed in Figure 5a at different delay times for all possible combinations of the four experiments. A positive correlation is seen at all delay times except at 8 and 64 μs, which show a more random orientation of the residuals. A similar plot is displayed for the two-exponential fit, Figure 5b, which shows the lack of correlation between the residuals at all time delays. The scatter of the points is due, very likely, to the small offsets in the residuals. Subtracting the correlation values shown in Figure 5b from the ones shown in Figure 5a is likely to correct for the offsets seen in Figure 5a. The resulting improved correlation plot is displayed in Figure 5c, and indeed it shows a much smaller range of scatter and a very clear picture of correlation between the different experiments. The shape of the correlation plot also carries very important information regarding the global exponential fit. The absence of correlation at 8 and 64 μs delay times is a strong indication of the need for two exponentials in the fit. This point is illustrated in Figure 6. The solid curve shows the calculated concentration of an intermediate decaying in two consecutive steps with 12 and 180 μs lifetimes. The dashed curve superimposed on it represents the best single-exponential fit with a 200 μs decay time. It is seen very clearly that the two curves intercept at two delay times. At these two delay times the single-exponential fit provides the same quality of fit as the two-exponential one. The residuals of the single-exponential fit at those two time delays thus have the same level of correlation as the residuals of the two-exponential fit, which is nearly zero. Therefore, the values and the shape of the correlation plot in Figure 5a,c show that a single exponential does not fit the experimental data adequately and all individual experiments require a second exponential to be included in the global exponential fit.

DISCUSSION

Traditionally the Lumi intermediate has appeared to be an island of stability in the rhodopsin bleaching sequence. At low temperatures Lumi is stable over a wide temperature range (*4*) and near-physiological temperature absorbance changes were so small, from 1 μs to tens of microseconds, that interest and measurements tended to focus on other time ranges where much larger spectral changes occurred. The imperturbable nature of Lumi was further underscored by the fact that it was the last intermediate whose properties were unaffected by detergent solubilization. This latter phenomenon interfered with high signal-to-noise ratio studies of Lumi decay until more recently when these detergent effects were better understood. Even so, a small absorbance change such as is reported here must always be viewed skeptically because of the possible presence of artifacts of comparable size. However, recent results have found kinetic components on the 10 μs time scale in certain artificial rhodopsins with synthetically modified retinylidene chromophores (*10*), and previously changes on this time scale were seen in a rhodopsin mutant related to those artificial pigments (*9*). The current work was undertaken because it was suspected that a similar component might exist in rhodopsin.

Absorbance Change Is neither Rotational Diffusion nor Isorhodopsin Relaxation. The primary artifact expected in rhodopsin on this time scale is rotational diffusion of rhodopsin in membrane (*11*), and hence detergent-solubilized samples were used here. As is clear from Figure 3, no oriented population exists on the time scale of these measurements. Further, the identical results obtained for the fast Lumi decay component in the two detergent concentrations studied here imply that heterogeneity of rhodopsin's environment in detergent suspensions does not account for the appearance of a fast component. Analysis of data previously collected from membrane suspensions of rhodopsin (*6*, *12*) supports the idea that an identical component is present in those measurements and, thus, is a property of rhodopsin even in membrane. The primary feature in the polarized membrane measurements distinguishing between a rotational artifact and real spectral change associated with a photointermediate is the fact that perpendicularly polarized probe light measurements showed a decay of the fast component (as seen here for a real photointermediate) rather than a growing in as would be expected from rotational relaxation of an oriented population of rhodopsin and lumirhodopsin. In other words, both parallel and perpendicularly polarized probe light in membrane show a similar decaying fast component rather than displaying fast components of opposite sign as they should if the origin of the component were only rotational diffusion. Thus, reinterpretation of the membrane data that showed a fast component, collected under conditions which should have been blind to rotational diffusion, supports the idea that a similar Lumi evolution is occurring there. Evidence for this position comes from the similar shapes and apparent rate of the fast component found here and that found in membrane suspensions of rhodopsin (*12*).

Another possible problem for assigning the absorbance changes seen here to Lumi is that they arise instead from relaxation of the isorhodopsin always formed to some degree in photolysis experiments. Difference spectra collected on shorter time scales have shown that the bulk of the absorbance change between rhodopsin and isorhodopsin takes place on the subnanosecond time scale [compare the data reported in Einterz et al. (*17*) to that in Hug et al. (*5*)], but the possibility exists that a small part of that spectral relaxation is delayed and could appear on the time scale studied here. We thus compared the results obtained from rhodopsin excitation using 540 nm light with those from 477 nm excitation since nanosecond pulses of 540 nm light produce far more isorhodopsin (~3 times as much in this case) due to their more efficient secondary photolysis of bathorhodopsin. The identical results obtained for the fast kinetic component using 477 and 540 nm excitation (data not shown) led us to conclude that isorhodopsin relaxation is not a contributing factor and that the origin of the fast component is likely to be a structural change from an early form, Lumi I present at 1 μs, to a second red-shifted form, Lumi II, with a time constant of 12 μs.

Figure 4 shows other changes accompanying Lumi II formation in addition to the ~2 nm red shift in the absorbance maximum. Lumi II appears to have a slightly smaller extinction coefficient in the main absorbance band and a somewhat larger one in the so-called cis band region (near 350 nm). As shown in the inset of Figure 4, the peak of the Lumi II minus Lumi I difference in the near-ultraviolet (heavy line) appears to be shifted from the 380 nm maximum of Meta I_{380} in the scaled plot of b_2 (fine line). Changes in the cis band region could be caused by changes in chromophore torsion that take place in the Lumi I → Lumi II transition. Similarly, torsion changes are also likely to affect the main band extinction coefficient. However, significant noise exists in the difference spectrum, and it is possible that some formation of a 380 nm absorber takes place during the decay of Lumi I.

Character of the 12 μs Absorbance Change. One might ask whether the observations described here justify the conclusion that we have discovered a new rhodopsin photointermediate. There is a long history of interpretation of optical absorbance changes in terms of intermediate species. The term rhodopsin bleaching sequence refers to the prephotometric observation that changes in optical absorbance properties accompany visual excitation. The ability to thermally trap species which also appear in time-dependent measurements has traditionally been taken as evidence that functionally important intermediates can appear in both kinds of studies. Optical absorbance measurements remain important in revealing new intermediates because optical methods have an advantage in time resolution compared to other spectroscopies and, where a suitable chromophore is present, have sensitivity advantages as well. Although there are limits to the information content of optical absorption techniques, in combination with other spectroscopies, they can be used to discover structural details of intermediates which occur along activation pathways or cycles. Application of other techniques can be critical for a full understanding, as was the case for bathorhodopsin whose torsionally strained nature was revealed by resonance Raman spectroscopy (*18*) after conditions stabilizing it had been determined in low-temperature optical absorbance studies (*19*). In other cases absorption measurements alone have been sufficient to provide an understanding of the difference between two intermediate species. An example of such a case is the red-shifted, early form of bathorhodopsin, sometimes referred to as photorhodopsin, that is now understood as a vibrationally excited form of bathorhodopsin. On the femtosecond time scale such red shifts and relaxations are now recognized to be a fairly ubiquitous phenomenon after photoexcitation. Even though such species would probably not be separately named intermediates now, prior to this understanding the term photorhodopsin was a useful term for organizing research into the phenomenon. However, except for this particular case of thermal deexcitation, other "unrelaxed" species probably coincide with what are thought of as intermediates. In general, the unrelaxed dimension is of interest in structural and mechanistic terms.

While a clear distinction can be made between true intermediates and an isoform like isorhodopsin, the difference between two intermediates and two substates of a single intermediate is less clearly defined. In mechanistic terms, a substate may be thought of as a side branch off a main reaction sequence. Two categories of substates exist. One, the fast case, occurs when the side branch comes to equilibrium faster than the formation rate of the intermediate, and the other, a slow case, occurs when the substate equilibrium is established slower than the intermediate's formation rate. In the former, fast substate case, the substates

will be intrinsically harder to characterize structurally and may be of little interest as distinct species because the energetic barriers between them are smaller than the energy barriers between "true" intermediates. On the other hand, species which correspond to the slow substate case can at least in principle be independently characterized structurally and hence have importance for a mechanistic understanding of the system. While it has not yet been determined whether Lumi I and Lumi II are distinct main line intermediates or slow substates of a single intermediate, the existence of two states must be distinguished in order for other spectroscopic techniques to be correctly applied because, depending on the conditions of measurement, Lumi II either will or will not be present. On the basis of its being a reproducible and at least potentially a well-defined phenomenon along the rhodopsin activation pathway which merits further study in other laboratories, Lumi II merits the status of a named intermediate.

Absorbance Changes on Similar Time Scales Occur in Rhodopsin Mutants. On the basis of previous results from unmodified rhodopsin, the fastest process expected on the time scale studied here would be the initial phase of the decay of Lumi to form Meta I_{380}, a process which speeds up as detergent disrupts the membrane, but whose limiting short lifetime is 120 μs in purified rhodopsin samples (*13*). However, absorbance changes on the same time scale as the 12 μs process seen here in rhodopsin have been observed previously in artificial visual pigments and in at least one rhodopsin mutant. After photolysis of 5-ethylisorhodopsin, a Lumi decay with a lifetime of 8 μs was observed. The time scale of the change observed here in rhodopsin is also similar to a Lumi decay with a lifetime of 14 μs seen after photolysis of the rhodopsin mutant G121A. The similarity of Lumi decay behavior in 5-ethylisorhodopsin and G121A rhodopsin also extends to the behavior of the intermediates preceding Lumi, which is interesting because the rhodopsin crystal structure places an Ala121 methyl group very near to where the C5 methyl group of the chromophore is presumably located. The spectral shift accompanying the fast Lumi decay in those two cases is to the blue, producing a photointermediate that absorbs near 475 nm, and for that reason the decay product of Lumi was originally assigned to Meta I_{480}. At the time of those experiments, formation of Meta I_{480} seemed unusual because both preparations were detergent suspensions, and rhodopsin fully solubilized in detergent produces little or no Meta I_{480} (*13*), making it difficult to understand why Meta I_{480} was favored and formed faster after photolysis of 5-ethylisorhodopsin and G121A rhodopsin under similar conditions. In light of the current results, an alternative assignment of the product of Lumi decay in those two cases seems preferable i.e., a Lumi II whose spectrum is perturbed by the similarly placed bulky substituents. It would not be surprising if the addition of a methyl group on the helix III side of the β-ionone ring shifted the spectrum of one or more photointermediates because bulk at that position should affect torsion around the C6−C7 bond which is known to affect the absorbance spectrum of visual pigments (*20*). Given that BSI formation is believed to impart a twist in the C6−C7 bond in the same sense to that which would be produced by a bulky substituent on the helix III side of the ring (*21*), it is plausible that the modifications in 5-ethylisorhodopsin and G121A rhodopsin further reduce planarity of the chromophore. If this is the case, structural changes associated with formation of Lumi II presumably involve a change in the protein which releases a constraint on the opposite side of the β-ionone ring from helix III, allowing more C6−C7 bond torsion after photolysis of 5-ethylisorhodopsin and G121A rhodopsin than occurs in the corresponding stage after photolysis of unmodified rhodopsin. Exaggeration of C6−C7 torsion at Lumi II as an explanation of the anomalous blue shift in the case of 5-ethylisorhodopsin and G121A is consistent with the fact that a Lumi decay with a lifetime of 27 μs was observed after photolysis of a bicyclic isorhodopsin analogue which produced a red-shifted product as is seen here for rhodopsin. In the case of the bicyclic isorhodopsin analogue, a six-membered ring constrains rotation around the C6−C7 bond.

The fact that a change takes place at the ring end of the chromophore in Lumi is of interest because recent resonance Raman results (*7*) have revealed unusual PSB hydrogen-bonding changes at Lumi. The model proposed on the basis of those measurements shows that at Lumi the PSB hydrogen bond has been broken and has not re-formed. Such an unstable structure near the PSB seems incompatible with the previous notion that Lumi is an island of stability. The current picture based on the results presented here involving two Lumi intermediates allows the unstable structure to be more transient and reveals more detail about the apparently complex motion of the chromophore leading up to PSB deprotonation. Photolabeling experiments support the idea that a large change in ring position has occurred at the Lumi stage (*8*).

Conclusion. The data at 20 °C reported here show that a small but definite red shift of the lumirhodopsin spectrum takes place with a time constant of 12 μs in detergent suspensions. The size of this component relative to the others seen in absorbance measurements is small since the spectra of Lumi I and Lumi II are very similar. The small size of this kinetic component contributed to its late discovery, but it is important to note that the significance of this process cannot be assumed to be proportional to its size. From what is already known about rhodopsin activation, the lumirhodopsin time scale is a very interesting one during which the SB hydrogen-bonding environment is changing and, at physiological temperatures immediately preceding SB deprotonation, is a critical factor in activation. Further, a fast process similar to that seen here in detergent has been seen in membrane suspensions of rhodopsin (*12*), but the possibility of transient absorbance changes on the microsecond time scale due to rotational diffusion of rhodopsin in the membrane and the similarity of its spectral shape to that expected from rotation of rhodopsin photoproducts in membrane made its detection there ambiguous. It is now clear that a real absorbance change takes place on this time scale both in detergent and in membrane and that the process involved is the jumping off point for SB deprotonation under physiological conditions.

ACKNOWLEDGMENT

The authors acknowledge co-workers Thorgeir Thorgeirsson and Stefan Jäger, who in the data they collected on membrane suspensions of rhodopsin recognized and argued for the significance of the fast component characterized here in detergent suspensions.

REFERENCES

1. Palczewski, K., Kumasaka, T., Hori, T., Behnke, C. A., Motoshima, H., Fox, B. A., Le Trong, I., Teller, D. C., Okada, T., Stenkamp, R. E., Yamamoto, M., and Miyano, M. (2000) *Science 289*, 739−745.
2. Okada, T., Ernst, O. P., Palczewski, K., and Hofmann, K. P. (2001) *Trends Biochem. Sci. 26*, 318−324.
3. Okada, T., Fujiyoshi, Y., Silow, M., Navarro, J., Landau, E. M., and Shichida Y. (2002) *Proc. Natl. Acad. Sci. U.S.A. 99*, 5982−5987.
4. Yoshizawa, T., and Shichida, Y. (1982) *Methods Enzymol. 81*, 333−354.
5. Hug, S. J., Lewis, J. W., Einterz, C. M., Thorgeirsson, T. E., and Kliger, D. S. (1990) *Biochemistry 29*, 1475−1485.
6. Thorgeirsson, T. E., Lewis, J. W., Wallace-Williams, S. E., and Kliger, D. S. (1993) *Biochemistry 32*, 13861−13872.
7. Pan, D., Ganim, Z., Kim, J. E., Verhoeven, M. A., Lugtenburg, J., and Mathies, R. A. (2002) *J. Am. Chem. Soc. 124*, 4857−4864.
8. Borhan, B., Souto, M. L., Imai, H., Shichida, Y., and Nakanishi, K. (2000) *Science 288*, 2209−2212.
9. Jäger, S., Han, M., Lewis, J. W., Szundi, I., Sakmar, T., and Kliger, D. S. (1997) *Biochemistry 36*, 11804−11810.
10. Szundi, I., de Lera, A. R., Pazos, Y., Alvarez, R., Oliana, M., Sheves, M., Lewis, J. W., and Kliger, D. S. (2002) *Biochemistry 41*, 2028−2035.
11. Cone, R. A. (1972) *Nat. New Biol. 236*, 39−43.
12. Jäger, S., Szundi, I., Lewis, J. W., Mah, T. L., and Kliger, D. S. (1998) *Biochemistry 37*, 6998−7005.
13. Szundi, I., Mah, T. L., Lewis, J. W., Jäger, S., Ernst, O. P., Hofmann, K. P., and Kliger, D. S. (1998) *Biochemistry 37*, 14237−14244.
14. Oprian, D. D., Molday, R. S., Kaufman, R. J., and Khorana, H. G. (1987) *Proc. Natl. Acad. Sci. U.S.A. 84*, 8874−8878.
15. Lewis, J. W., and Kliger, D. S. (2000) *Methods Enzymol. 315*, 164−178.
16. Szundi, I., Lewis, J. W., and Kliger, D. S. (1997) *Biophys. J. 73*, 688−702.
17. Einterz, C. M., Lewis, J. W., and Kliger, D. S. (1987) *Proc. Natl. Acad. Sci. U.S.A. 84*, 3699−3703.
18. Palings, I., Pardoen, J. A., van den Berg, E., Winkel, C., Lugtenburg, J., and Mathies, R. A. (1987) *Biochemistry 26*, 2544−2556.
19. Yoshizawa, T., and Wald, G. (1963) *Nature 197*, 1279−1286.
20. van der Steen, R., Biesheuvel, P. L., Mathies, R. A., and Lugtenburg, J. (1986) *J. Am. Chem. Soc. 108*, 6410−6411.
21. Lewis, J. W., Fan, G.-B., Sheves, M., Szundi, I., and Kliger, D. S. (2001) *J. Am. Chem. Soc. 123*, 10024−10029.

BI0206964